BNL-20478

BROOKHAVEN NATIONAL LABORATORY
Associated Universities, Inc.
Upton, New York

ISA 75-10

ACCELERATOR DEPARTMENT
Informal Report

ISABELLE RING STRUCTURE AND PERFORMANCE

M. Month

July 8, 1975

ABSTRACT

A summary of the ISABELLE Ring Structure is presented. A phased approach to ISA operation is detailed. The initial performance potential is such as to allow p-p collisions at a wide range of energies and with unequal energies in the two beams. The quasi 8-fold periodicity could be broken to allow a hi-luminosity set-up. This could be achieved by small changes in the insertion quadrupole strengths. A discussion of future ISA phases is given. These would require the alteration of the physical layout of the insertions for various special experimental conditions.

1. Introduction

The proton-proton storage accelerator facility proposed consists of two intersecting magnet rings located side by side in a common tunnel. A cross section of the tunnel is shown in Fig. 1. Each of the superconducting magnets of each ring is contained in its own dewar and has its own separate mechanical support. The location and orientation of each magnet is thereby separately adjustable. A cross section of a dipole within its dewar is given in Fig. 2.

The circumference of each ring is 2960 m or 3 2/3 times the circumference of the AGS. The ring configurations are roughly circles broken by eight symmetrically placed insertions in which the beams are made to cross in their common median plane. The horizontally interlacing beams cross eight times, thus providing 8 areas for experimental exploitation. The two ISABELLE beams will be created from protons of kinetic energy 28.5 GeV accelerated in the AGS. They will be ejected ("single turn fast extraction") from the AGS into the beam line which is now feeding the North Area and the 7 ft bubble chamber and which would be extended to the proposed location of the ISA, shown in Fig. 3. On the scale of this figure, the ring separation (to be more accurate, the beam center separation), 75 cm, is not visible when compared to the mean ring radius, 471.1 m.

2. ISABELLE Magnet Configuration

The separated function ISABELLE lattice will have a standard configuration of quasi eight-fold periodicity. Each ring is comprised of 8 octants. Recall, however, that the rings interlace and therefore cross eight times. This implies that there are two types of octants: the inner arc octant and the outer arc octant. Thus, to be more precise, each ring consists of eight alternating inner and outer arc octants, four of each. Nonetheless, the main difference between inner and outer arcs is just in their bending geometry. The small ring separation of 75 cm has permitted a design in which the difference in focusing structure between inner and outer arcs is insignificant. This is in fact the basis for our designation of the design as quasi 8-fold periodic.

Each inner and outer arc octant consists of:

Regular Bending Cells	7/octant
Modified Bending Cells	3/octant
Straight Insertion	1/octant

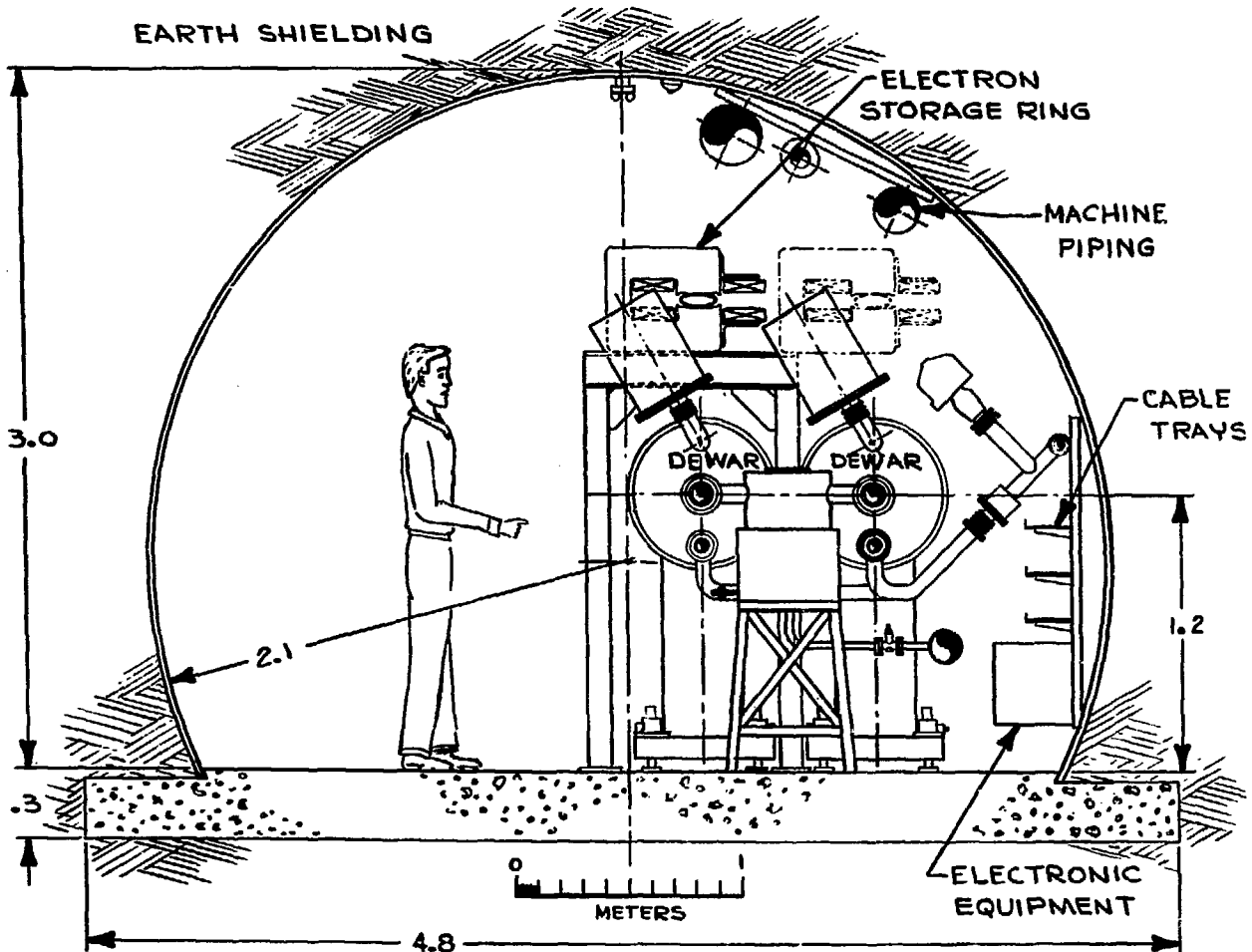

Fig. 1. ISABELLE tunnel cross section.

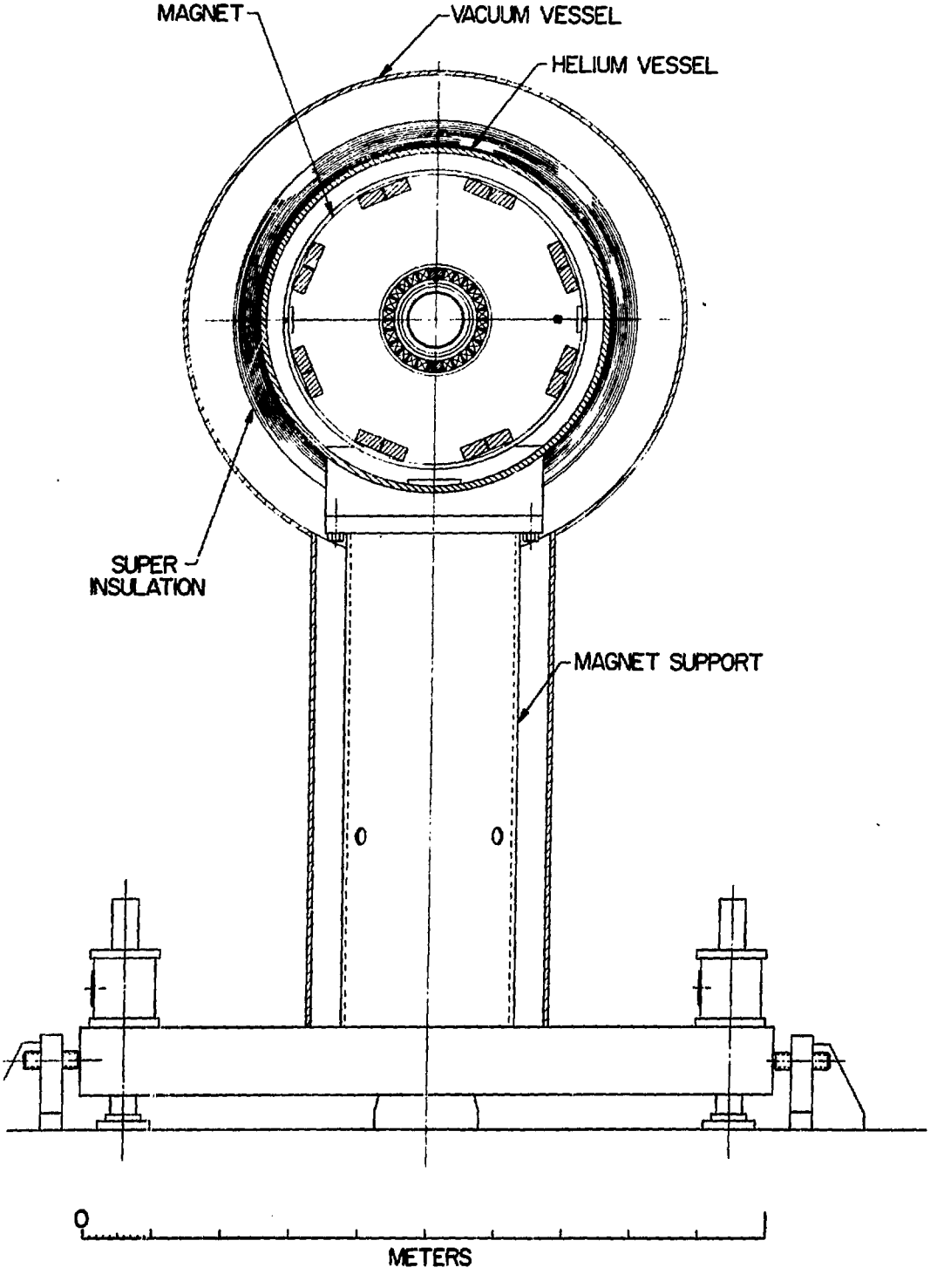

Fig. 2. Dipole dewar cross section.

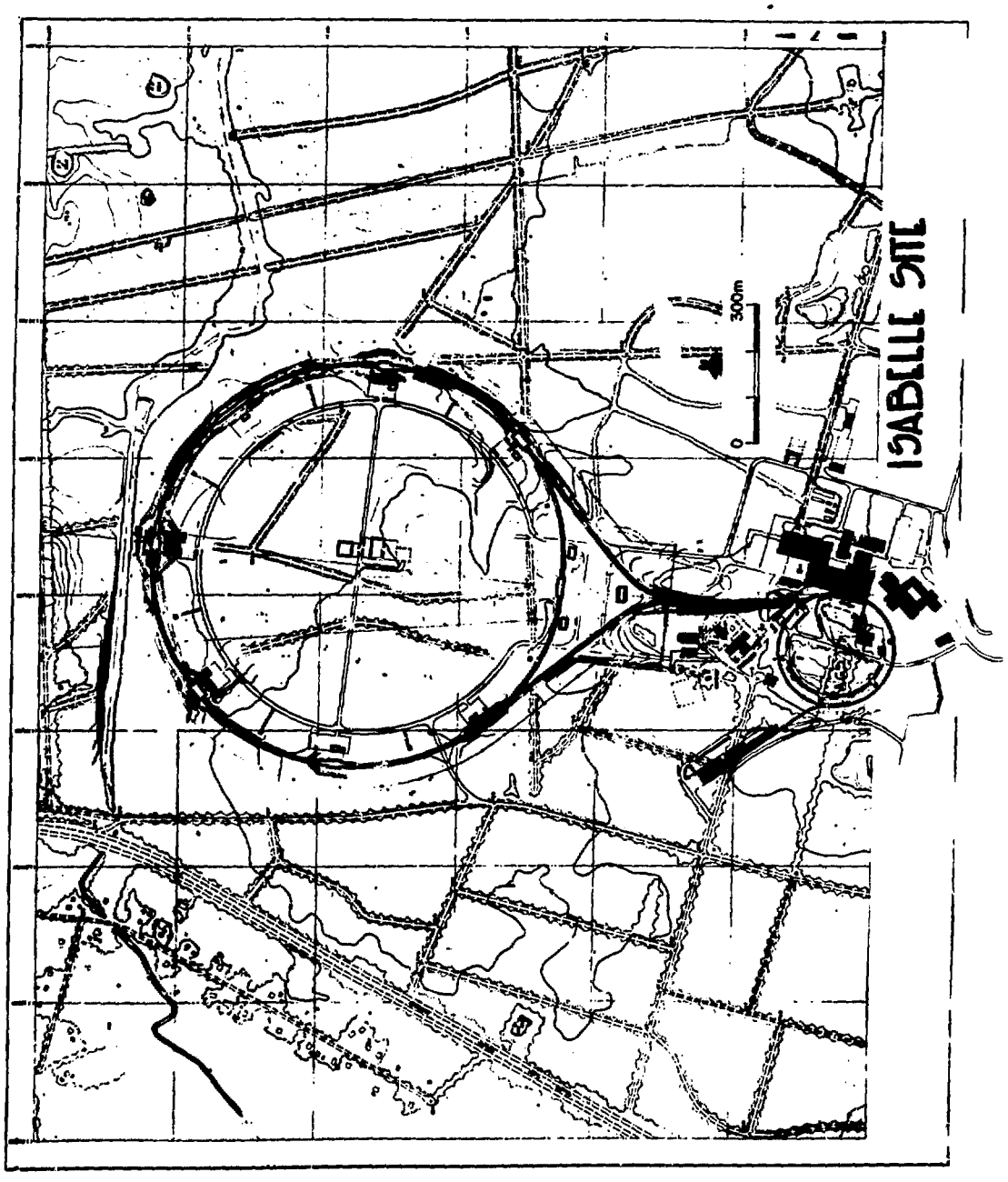

Fig. 3. ISA site plan.

The main part of the bending is done in the 56 regular bending cells. Each is a standard FODO cell consisting of 4 dipoles and 2 quadrupoles. The physical layout of a half cell is pictured in Fig. 4. The magnet positions and beam bending geometry are drawn in Fig. 5. Since the bending magnets in inner and outer arcs are designed to be identical (bending radius, 169.589 m; effective length, 4.11m; leading to a bending angle, 24.235 mrad), and we require the standard separation of 75 cm to remain constant along the regular bending cell portions of the rings, then it follows that the inner arc regular bending cell must be slightly shorter than its outer arc counterpart. In fact, with the given bending magnet characteristics, to maintain the 75 cm separation requires that the inner arc cell, containing 4 bending magnets, be 7.27 cm shorter than the outer arc cell. Since the cell length in the outer arc is designed to be 25.4 m, this represents a rather insignificant difference of less than 0.3%.

A small portion of the bending in the two rings is performed in the 3 modified bending cells adjacent to the straight insertion, 1½ on each side. These cells are essentially the same as the regular bending cells in terms of their focusing structure. The bending magnets, however, are arranged so that the beams begin to converge towards each other as they head for the collision point. The beam trajectories in the straight insertions and the 3 adjacent modified bending cells for both inner and outer arc geometries are depicted in Fig. 6.

Before converging, the horizontal separation of the beams is 75 cm, providing sufficient space to accommodate separate dewars for each individual magnet. In the modified bending cells, as the beams begin to converge, we have taken for the minimum dipole dewar enclosure, 70 cm. As can be seen in Fig. 6, the beam separation is sufficient so that all dipoles can be placed in separate dewars. The dewar enclosures for quadrupoles are smaller, about 50 cm. Thus, quadrupoles can be placed in separate dewars, except close to the collision point. Quadrupoles are required close to the collision point to focus the rapidly enlarging beam width. Our design in fact requires the first focusing magnet to be located at a point where the beams are separated by 22.8 cm, a space considerably smaller than is required if we are to have separate magnets for each beam, with each enclosed in its separate dewar. However, by designing long magnets with maximum gradients of 4 kG/cm for the quadrupole doublet system close to the collision point

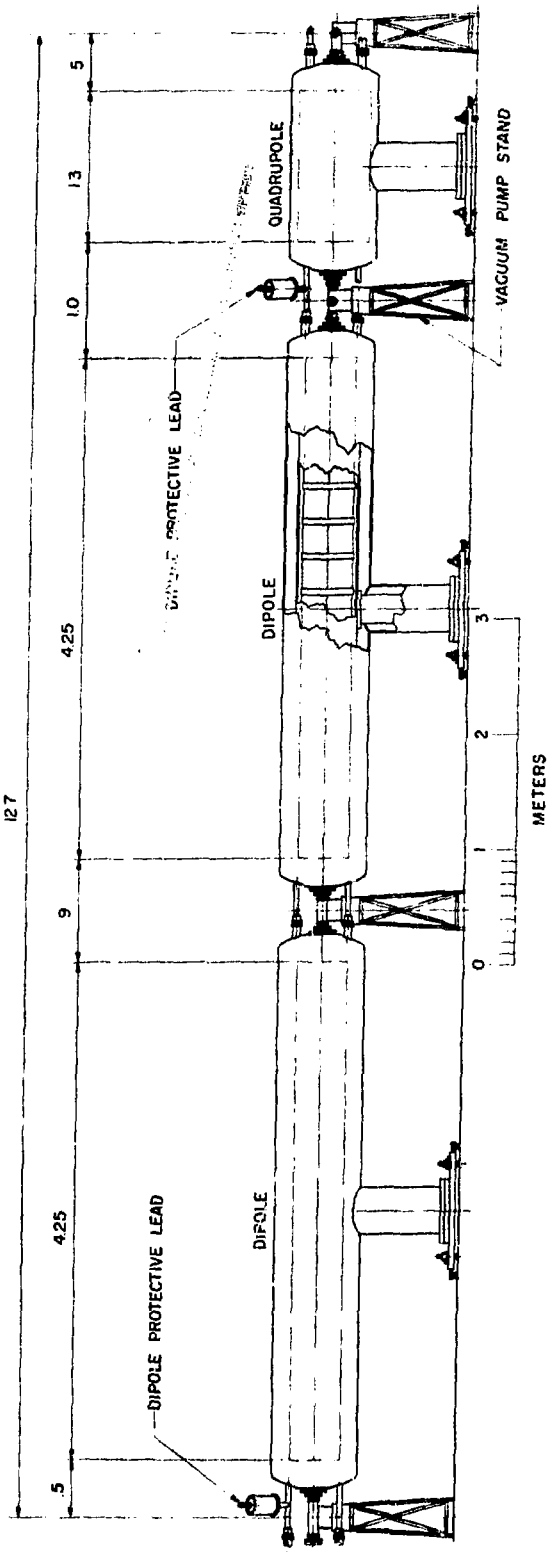

Fig. 4. Regular half cell.

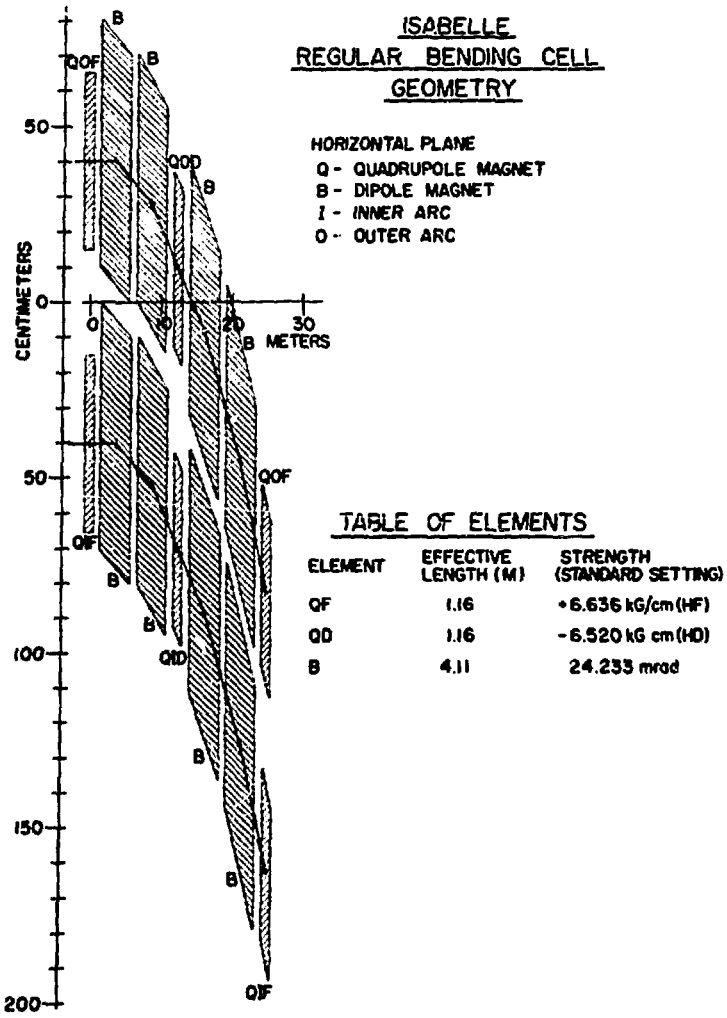

Fig. 5. Beam trajectories in inner and outer arc regular bending cells. The transverse limit of each magnet includes its dewar enclosure. The origin of the coordinate system is at a point mid-way between the inner and outer arc central orbits at a focusing quadrupole. The X-axis is a line through the coordinate system origin, parallel to the orbit trajectories. The Y-axis is a line perpendicular to the X-axis through the origin.

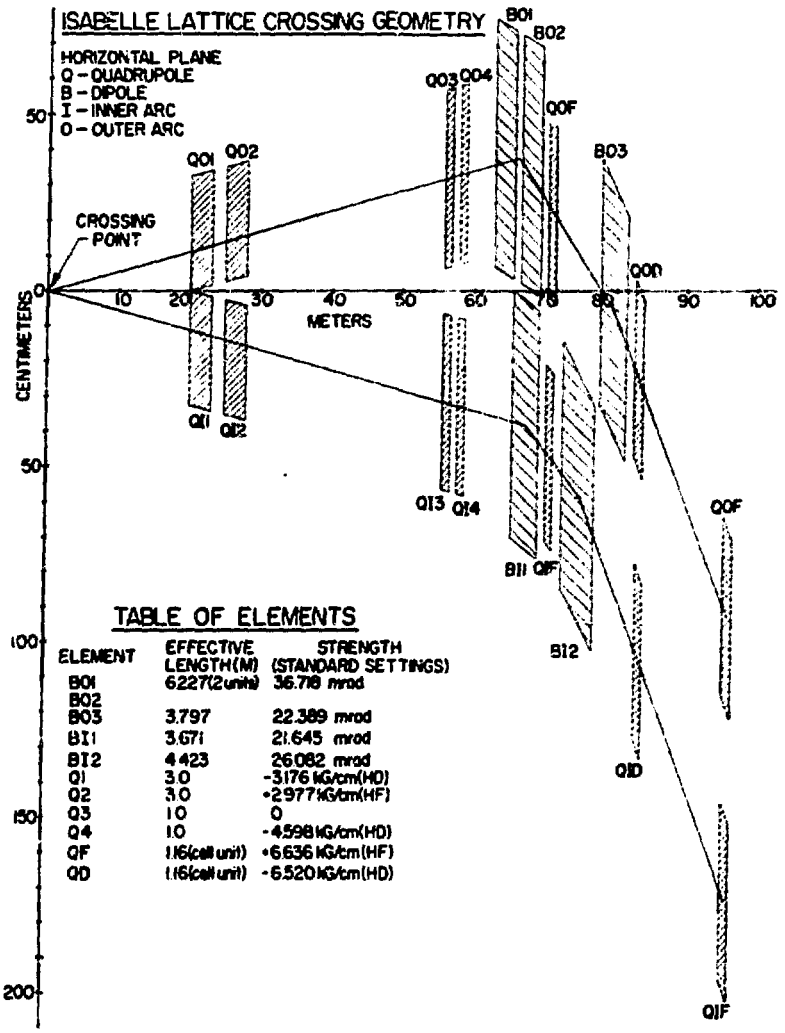

Fig. 6. Beam trajectories in the crossing region. The transverse limit of each magnet includes dewar enclosure.

the amount of superconducting coil width and iron shield width can be made sufficiently small so that the separation of 22.8 cm can accommodate separate magnets. The idea is then to enclose the inner and outer arc pair in a combined dewar. We then have for the quadrupole focusing doublet: separate magnets, combined dewar. The magnet support structure must be specially constructed to give sufficient independent control over the location of each magnet in the combined dewar.

The collisions take place at the insertion center where there is ± 20 m of free space provided for experimental apparatus. There is another long free space of about 28 m on each side of the collision point but following the first focusing doublet. This space will to some extent be available for experimental measurement and detection equipment. However, these straight sections will to a large extent be used for equipment needed for various machine functions, in particular, beam injection and ejection, rf systems, special multipole magnets, beam diagnostic systems, and beam scrapers. In addition, this space can be used for magnets capable of directing into one of the beam channels an electron beam, thus providing e-p collisions.

The rings in the standard configuration are designed so as to be completely electrically and magnetically independent. This feature means that the standard operation includes experiments with the two beams at unequal energies. It also means that antiprotons can circulate in one ring with protons in the other, thus providing p-$\bar{p}$ collisions, with no geometrical constraints.

Figure 7 is a scaled drawing of the ISABELLE octant, both inner and outer arc configurations. Using the coordinate system defined in this figure, Table I lists the coordinates of all the magnets in the inner and outer arc octants.

3. The ISABELLE Lattice: The Characteristic Functions and Parameters

The characteristic lattice functions are the amplitude functions, β_h and β_v, and the horizontal dispersion function, X_p. Since the beam trajectories for both rings are in the same median plane, there is no vertical bending and the vertical dispersion function, $Y_p=0$. All these functions are plotted in Fig. 8. A schematic of the corresponding magnet configuration is also shown. Since each octant has a center of symmetry, it is necessary only to show half an octant. Actually, only 2 regular bending cells of the required 3½ to form half an octant

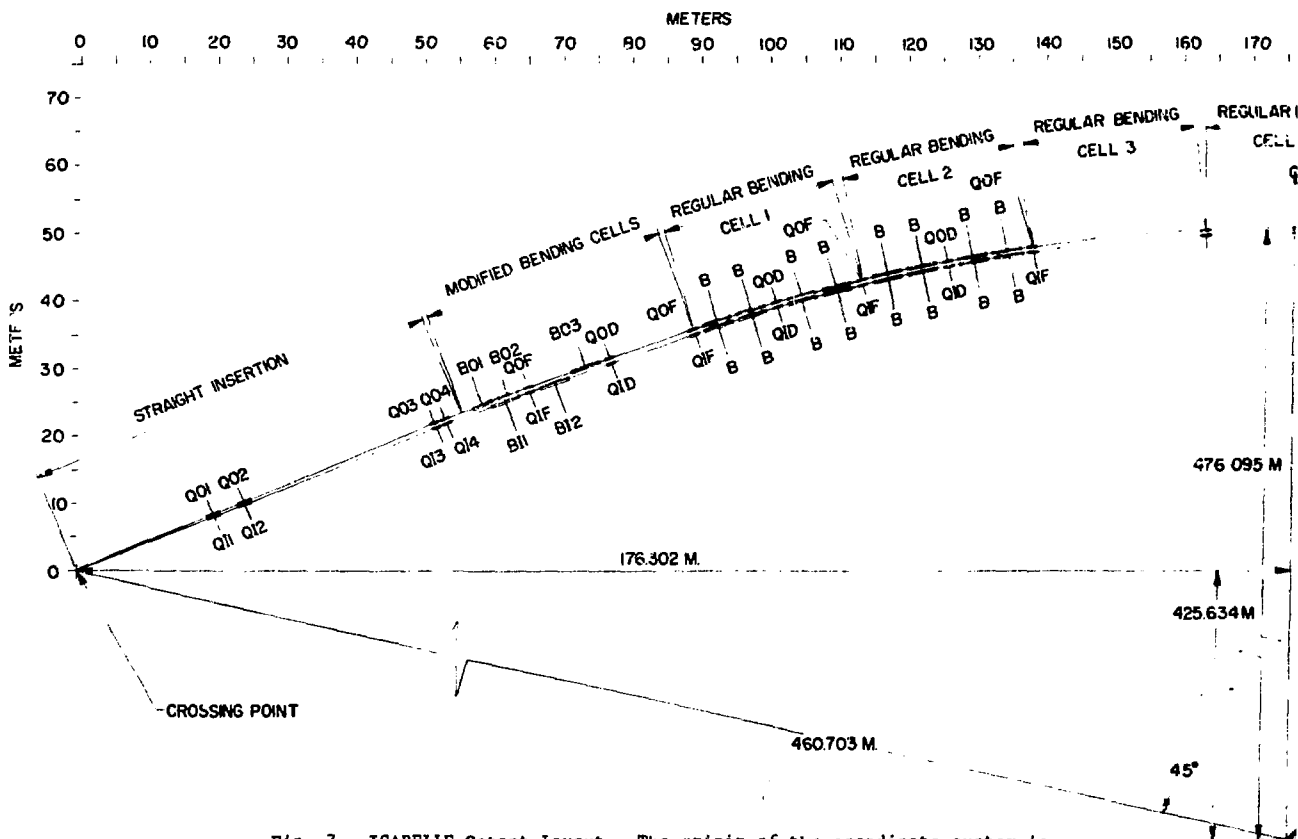

Fig. 7. ISABELLE Octant Layout. The origin of the coordinate system is located at a crossing point. The X-axis is a line joining two consecutive crossing points. The Y-axis is a line perpendicular to the X-axis through the origin.

ISABELLE OCTA

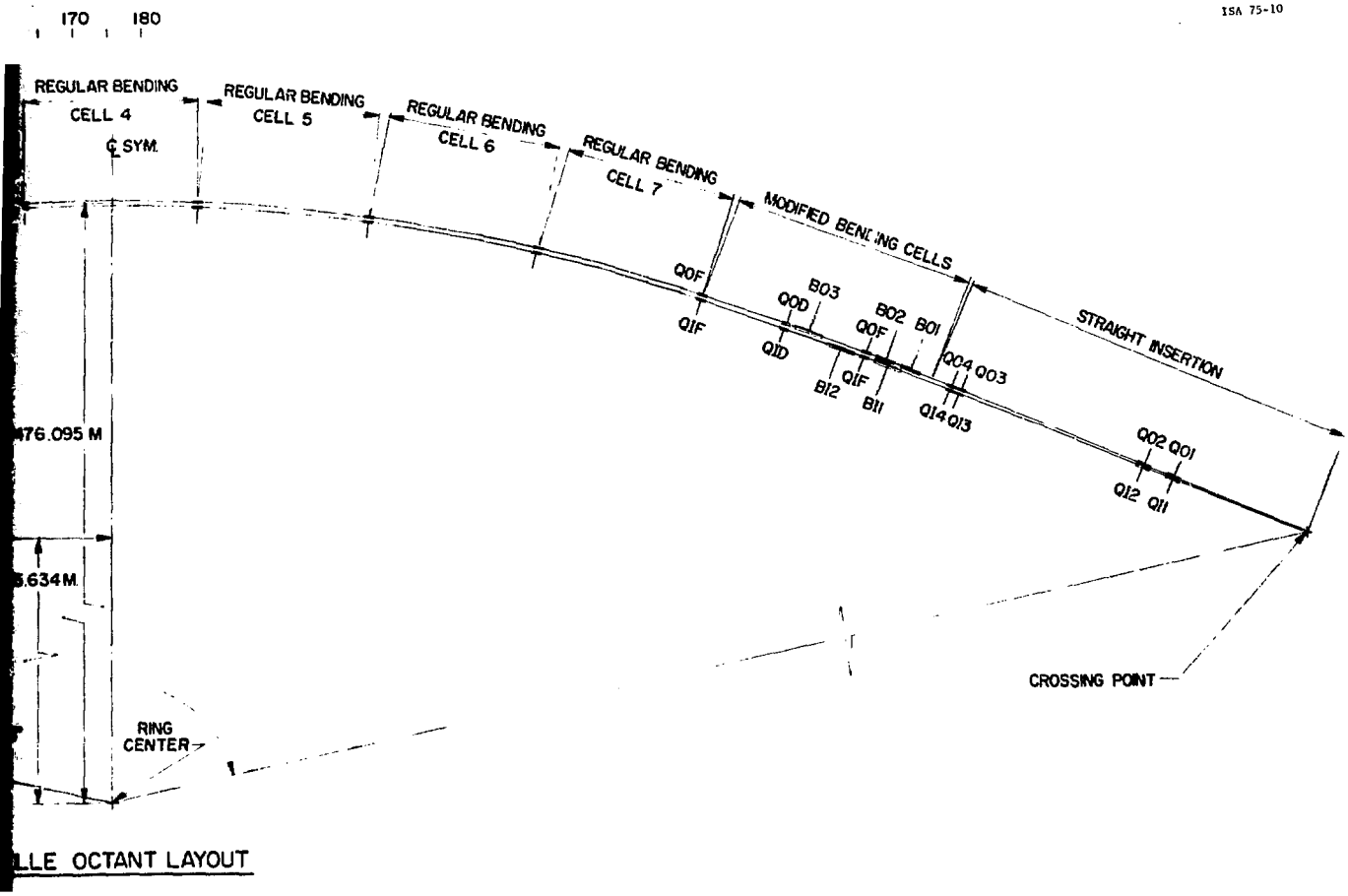

LLE OCTANT LAYOUT

2

TABLE I

Magnet Coordinates for an ISA Octant From Crossing Point To Center of Symmetry

The coordinate system center is at the location of a crossing point. The X-axis is the line joining two crossing points and the Y-axis is a line perpendicular to the X-axis.

Magnet (Inner Arc)		X	Y
St. Insertion	QI1	19.909	8.115
	QI2	24.438	9.960
	QI3	52.367	21.343
	QI4	53.756	21.909
Modified Bending Cell	BI1	62.151	25.331
	QIF	64.464	26.097
	BI2	69.144	28.006
	QID	77.411	30.923
	QIF	89.384	35.150
Regular Bending Cell 1	B	92.945	36.406
	B	97.824	38.023
	QID	101.432	39.103
	B	105.040	40.183
	B	109.991	41.551
	QIF	113.647	42.455
Regular Bending Cell 2	B	117.303	43.359
	B	122.313	44.478
	QID	126.009	45.204
	B	129.704	45.929
	B	134.762	46.795
	QIF	138.488	47.341
Regular Bending Cell 3	B	142.215	47.886
	B	147.309	48.506
	QID	151.057	48.872
	B	154.805	49.235
	B	159.923	49.608
	QIF	163.686	49.792
	B	167.446	49.973
	B	172.576	50.092
	QID	176.344	50.092

Magnet (Outer Arc)		X	Y
St. Insertion	QO1	19.816	8.340
	QO2	24.323	10.237
	QO3	52.121	21.937
	QO4	53.503	22.519
Modified Bending Cell	BO1&2	60.680	25.540
	QOF	65.200	27.250
	BO3	73.694	30.463
	QOD	77.093	31.667
	QOF	89.068	35.894
Regular Bending Cell 1	B	92.642	37.151
	B	97.538	38.746
	QOD	100.987	39.055
	B	104.770	40.911
	B	109.738	42.267
	QOF	113.388	43.172
Regular Bending Cell 2	B	117.067	44.078
	B	122.095	45.192
	QOD	125.784	45.919
	B	129.503	46.647
	B	134.579	47.516
	QOF	138.299	48.062
Regular Bending Cell 3	B	142.049	48.609
	B	147.161	49.282
	QOD	150.903	49.595
	B	154.675	50.013
	B	159.811	50.387
	QOF	163.566	50.517
	B	167.352	50.753
	B	172.500	50.832
	QOD	176.260	50.832

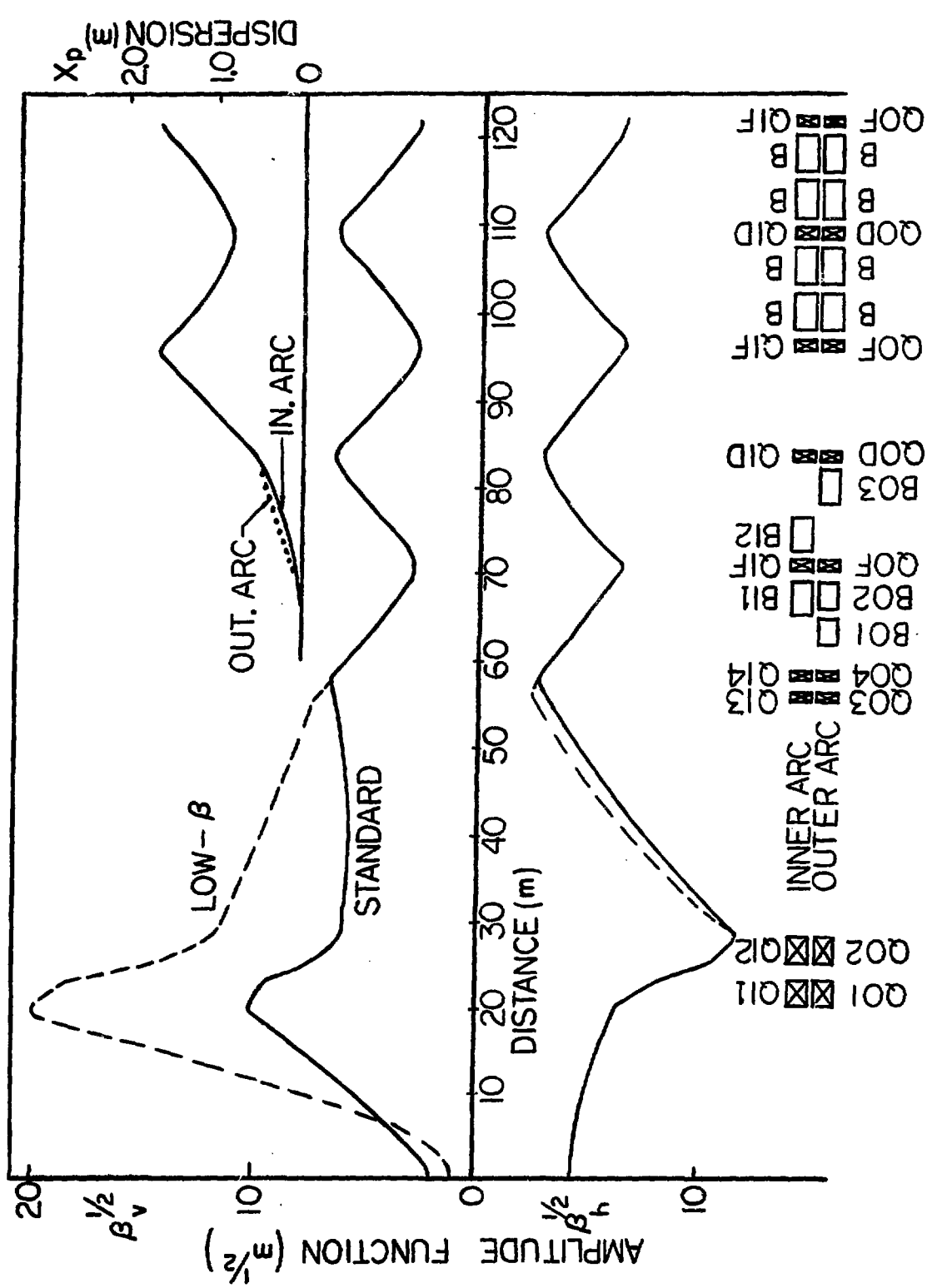

Fig. 8. ISA amplitude and dispersion functions, β_h, β_v and X_p. The β-functions for inner and outer arc configurations are indistinguishable on the given scale.

are shown. These are standard FODO cells and the characteristic functions are identical in each cell.

The β-functions in the insertion are matched to the values in the cells. To accomplish this, two quadrupole doublets on each side of the collision point are required. This quadrupole arrangement allows the change from standard to low-β configuration by a minor adjustment of the strength of the two doublets. The characteristic functions for the low-β matched insertion are also shown in Fig. 8. The low-β configuration has a β-value of 1 m at the crossing point compared to 4 m in the standard configuration. It is important to emphasize that the change from standard to low-β setups entails an increase in the peak value of β_v from 100 m in the standard arrangement to 400 m for low-β operation. This is not considered standard operation. It is not expected to be used in all insertions and special precautions will be taken in the construction and placement of the quadrupoles which are located at the nigh β_v values.

The horizontal dispersion function, sketched also in Fig. 8, is brought to zero in the modified bending cells, remaining zero throughout the straight insertion. Thus, the bending arrangement in these cells is seen to have a dual purpose. It not only provides the proper geometry for beam collision, as shown in Fig. 6, but this same bending configuration brings the dispersion function to zero in both inner and outer arcs. The importance of the 0 dispersion function in the crossing region lies in the fact that with the small crossing angle design for the ISA (more than an order of magnitude less than at the ISR) coupled with the large momentum spread required in all storage rings, a non-zero dispersion at the collision point would lead to a long interaction length. This is an undesirable characteristic because of the long range beam-beam electromagnetic interaction it creates and also because it complicates the analysis of experimental events. A non-zero dispersion function in the straight insertion would further complicate the β and dispersion matching and could create more stringent aperture requirements in the insertion quadrupoles.

The betatron matching can only be achieved at one central momentum. For off-momentum particles, a mismatch results. The primary effect on off-momentum particles is a tune shift. However, by applying high order multipoles, primarily

sextupoles, the tune variation with momentum can be removed. Since in order to sustain transverse beam stability from beam-environment interactions there must be a residual tune variation with momentum, i.e. a working line, these multipoles provide the necessary control of its shape. The main multipole correction is the sextupole term, which can be chosen to eliminate the natural lattice chromaticity (i.e. the linear variation of tune with momentum). The chromaticity, ξ, is defined as $\xi = p\, d\nu/dp$. In our standard lattice configuration, we have added sextupoles at the location of each quadrupole, to eliminate completely the chromaticity. There remains however a residual non-linear variation of tune with momentum, and this is plotted in Fig. 9. The residual can of course be removed with higher multipoles. However, there are other sources of tune variation with momentum which must also be included, in particular, single beam space charge effects. The result of multipole fields arising from these latter sources induce tune variations with momentum which are larger than the residual given in Fig. 9. Multipole correction strengths based on this residual alone are therefore not relevant.

Although the working line distortion, arising ultimately from the fact that off-momentum particles are mismatched in β-function, can be corrected with appropriate multipoles, the β-function mismatch itself cannot be eliminated. For the case of the standard insertion configuration, i.e. with $B_v^{max} \approx 100$ m, and with sextupoles added to remove the natural lattice chromaticity, we plot in Fig. 10 the variation of β with momentum at the crossing point, this variation being typical of the variation around the ring. It should perhaps be mentioned that one of our goals in designing the straight insertions was to limit the impact of these insertions on the β-variation across the momentum aperture. As can be seen, the β-variation is $\sim \pm$ 6% in the required $\pm$ 1% momentum aperture. The attainment of this rather small β-variation is primarily a result of our limitation on β to have a maximum value on the order of 100 m.

The main lattice parameters for the standard configuration are listed in Table II. Because of the long straight sections, the transition energy (in proton mass units) is not as close to the machine tune as it otherwise would be. In fact the machine tune ($\nu_h = \nu_v$), chosen to be $\sim$ 25.6, is 4 units larger than $\gamma_{tr} = 21.6$. These choices, although complex and interrelated, have been governed by the conflicting desires of 1) many [8] long straight sections, 2) a vacuum chamber of diameter no larger than 8 cm, and 3) a reasonable (low) stacking

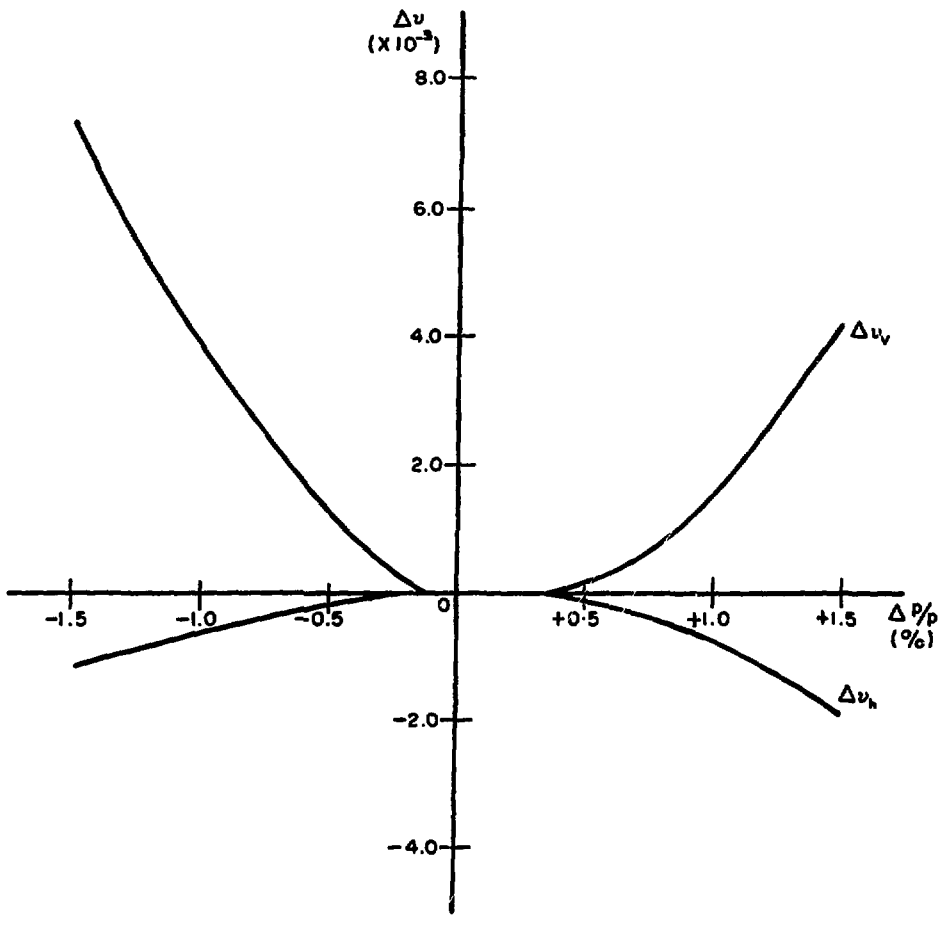

Fig. 9. Tune as a function of momentum. Residual tune after chromaticity correction with sextupoles. The central tunes are $\nu_h = \nu_v = 25.63$.

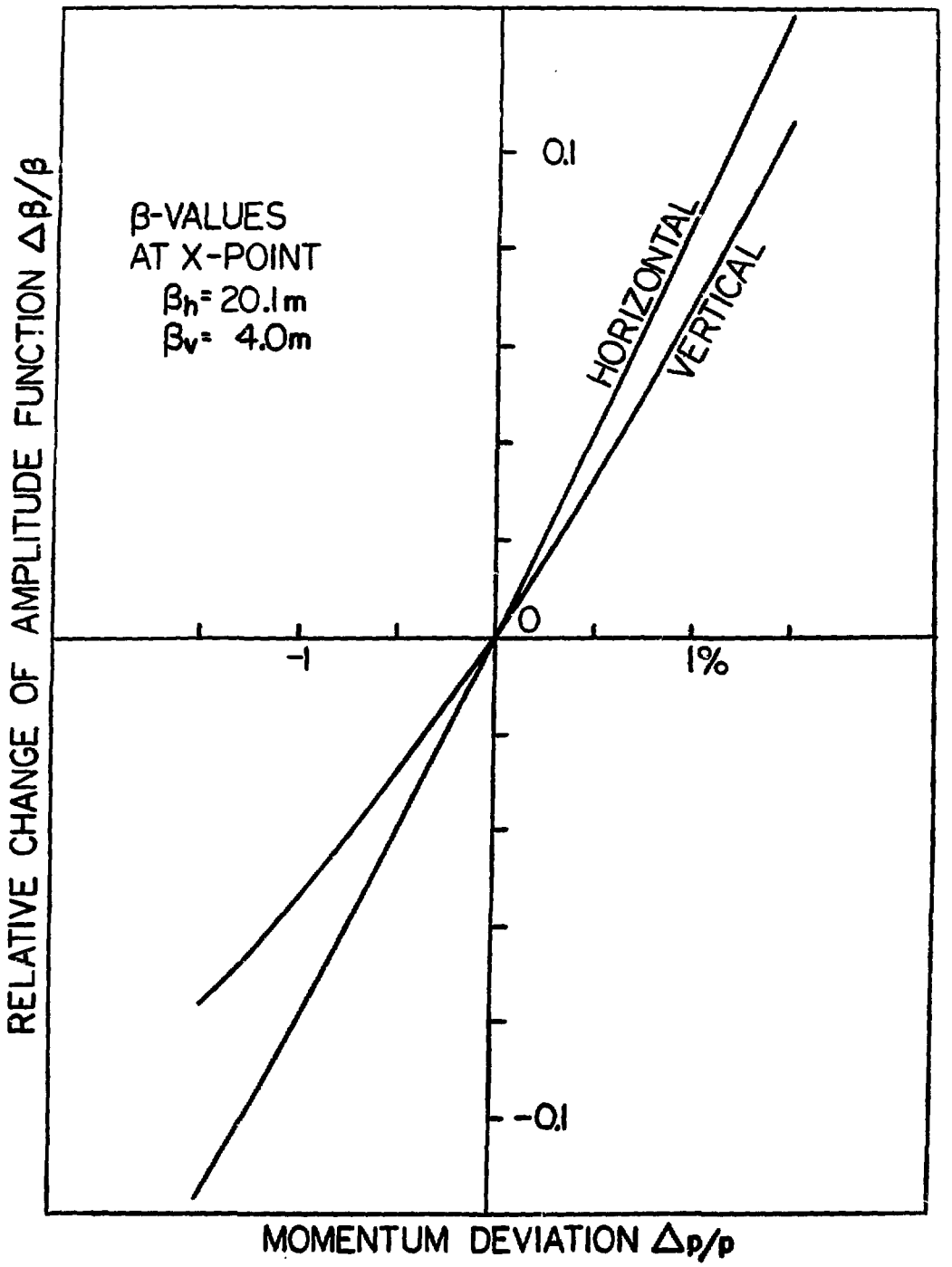

Fig. 10. β variation across the momentum aperture at the crossing point for the standard ISA lattice configuration. The maximum stack occupation is ± 0.8% for the bunched beam at 28.5 GeV. During stacking a maximum of 2% momentum aperture is required, more than half of which is required for the separation of the stack from the injected orbit.

TABLE II

ISA Ring Parameters

Energy (top)	200 GeV (γ = 213.2)
Energy (Injection)	29.5 GeV (γ = 31.4)
Circumference	2960 m (3 2/3 C_{AGS})
Average Radius	471.1 m
Magnetic Radius	169.6 m
Magnetic Field (E=200 GeV)	39.34 kG
Regular Cell Length	56 X 25.4 = 1422.4 m
Modified Cell Length	24 X 25.4 = 609.6 m
Straight Insertion Length	8 X 116.0 = 928.0 m
Ring Relationship	Horizontal
Separation of Central Orbits	75 cm
Tune ($\nu_v = \nu_h$)	25.63
Transition Energy (γ_{tr})	21.6
Chamber Aperture	± 4.0 cm

ISA Magnet Totals (per ring)

Number of Cell Quadrupoles (HF)	80
Number of Cell Quadrupoles (HD)	72
Number of Insertion Quadrupoles	64
Total number of Quadrupoles	216
Number of Cell Bending Magnets	224
Number of Special Bending Magnets	40
Total Number of Dipoles	264
Amplitude Function, β_{max} (cell)	42.7 m
Amplitude Function, β_{min} (cell)	7.7 m
Dispersion Function, $X_{p,\,max}$ (cell)	1.64 m
Dispersion Function $X_{p,\,min}$ (cell)	0.79 m
$\beta_{max,\,h}$ (Insertion, standard)	137.5 m
$\beta_{max,\,v}$ (Insertion, standard)	103.5 m

β_h^* (collision point)	20.2 m
β_v^* (collision point)	4.0 m
X_p (Insertions)	0.0
Y_p (Insertions and cells)	0.0
Natural Chromaticity ($\xi_h = pd\nu_h/dp$)	-38.9
Natural Chromaticity ($\xi_v = pd\nu_v/dp$)	-36.8
$\lvert\Delta\beta/\beta\rvert_{max}$ at $\Delta p/p = \pm 1\%$ (after correction with sextupoles)	± 6%

Sextupole Correction ($\rightarrow \xi = 0$ at $\Delta p/p = 0$)

Number of Sextupoles 2 × 56 = 112

Location of Sextupoles:

S_F, at HF Regular cell Quadrupoles-No. = 56

S_D, at HD Regular cell Quadrupoles-No. = 56

Sextupole Strength, $S = \int B'' \, d\ell/(Bp)$:

S_F	$0.151/m^2$
S_D	$-0.301/m^2$

Pole-tip Field, Sextupoles (at 6 cm radius):

B_F (pole, ℓ_s = 1.16 m, E = 200 GeV)	3.12 kG
B_D (pole, ℓ_s = 1.16 m, E = 200 GeV)	6.24 kG

time. 1) tends to make the circumference, C, large. If high currents are to be stacked in momentum space, implying a "large" momentum spread, then 2) tends to require a small dispersion function, X_p, in the lattice cells. Finally, 3) is directly correlated with a low transition energy, γ_{tr}. The conflict becomes clear when we note that the variables C, X_p, and γ_{tr} are related by

$$\frac{1}{\gamma_{tr}^2} = \frac{\int_o^C (X_p/\rho)\, ds}{C} \quad ,$$

where ρ is the magnetic radius of curvature [ρ = infinity if the dipole component is zero].

4. ISABELLE Performance

The basic ISA design is conceived as an extrapolation of the only existing set of p-p storage rings, the CERN ISR. Drawing upon the ISR experience, the ISA has been designed so as to have a superior performance potential. (1) By accelerating the stack, the ISA provides pp collisions over a large range of center-of-mass energies, 60 GeV to 400 GeV, as well as allowing independent energy setting in each beam from 30 GeV to 200 GeV. (2) With its small crossing angle and low-β characteristics the ISA can reach luminosities two orders of magnitude higher than the ISR, about 10^{33} cm^{-2} sec^{-1}. (3) The use of matched insertions allows the design of a stable lattice (stable over a sufficient momentum aperture) which has a long magnet-free straight section around the central collision point. In the standard ISA insertion design, ± 20 m can be used for experimental detection and measurement apparatus.

The operation of the ISA will proceed in phases. The initial performance characteristics are given in Table III. Starting from the standard quadrupole configuration, a small change in the strength of the vertically defocusing doublet at the entrance to the insertion leads straightforwardly to the low-β configuration, giving a luminosity of 5 × 10^{32} cm^{-2} sec^{-1} at 400 GeV c.m. To reach the design luminosity of 10^{33} cm^{-2} sec^{-1}, large aperture bending magnets as sketched in Fig. 11 are required to reduce the crossing angle from its standard value of 11.4 mrad to half this value, 5.7 mrad.

TABLE III

ISABELLE Performance - Initial Phase

	Standard	Standard Low Energy	Low-β	Low-β Low-Energy	Hi-Luminosity
Luminosity (cm^{-2} sec^{-1})	2.65×10^{32}	1.02×10^{32}	5.31×10^{32}	1.44×10^{32}	1.06×10^{33}
Tune Shift	1.74×10^{-3}	4.53×10^{-3}	8.68×10^{-4}	3.20×10^{-3}	1.74×10^{-3}
Crossing Angle (mrad)	11.38	11.38	11.38	11.38	5.69
Free Space (m)	± 20	± 20	± 20	± 20	± 13
$\ell_{INTERACTION}$(m)	± 0.19	± 0.50	± 0.19	± 0.50	± 0.38
β_v^* (m)	4.0	4.0	1.0	2.0	1.0
$\beta_{v,max}$ (m)	~ 100	~ 100	~ 400	~ 200	~ 400
β_h^* (m)	20	20	20	20	20
σ_v^* (mm,rms)	0.243	0.632	0.121	0.447	0.121
σ_h^* (mm,rms)	0.543	1.414	0.543	1.414	0.543
Energy (GeV)	200.0	29.4	200.0	29.4	200.0
Current (A)	10	10	10	10	10

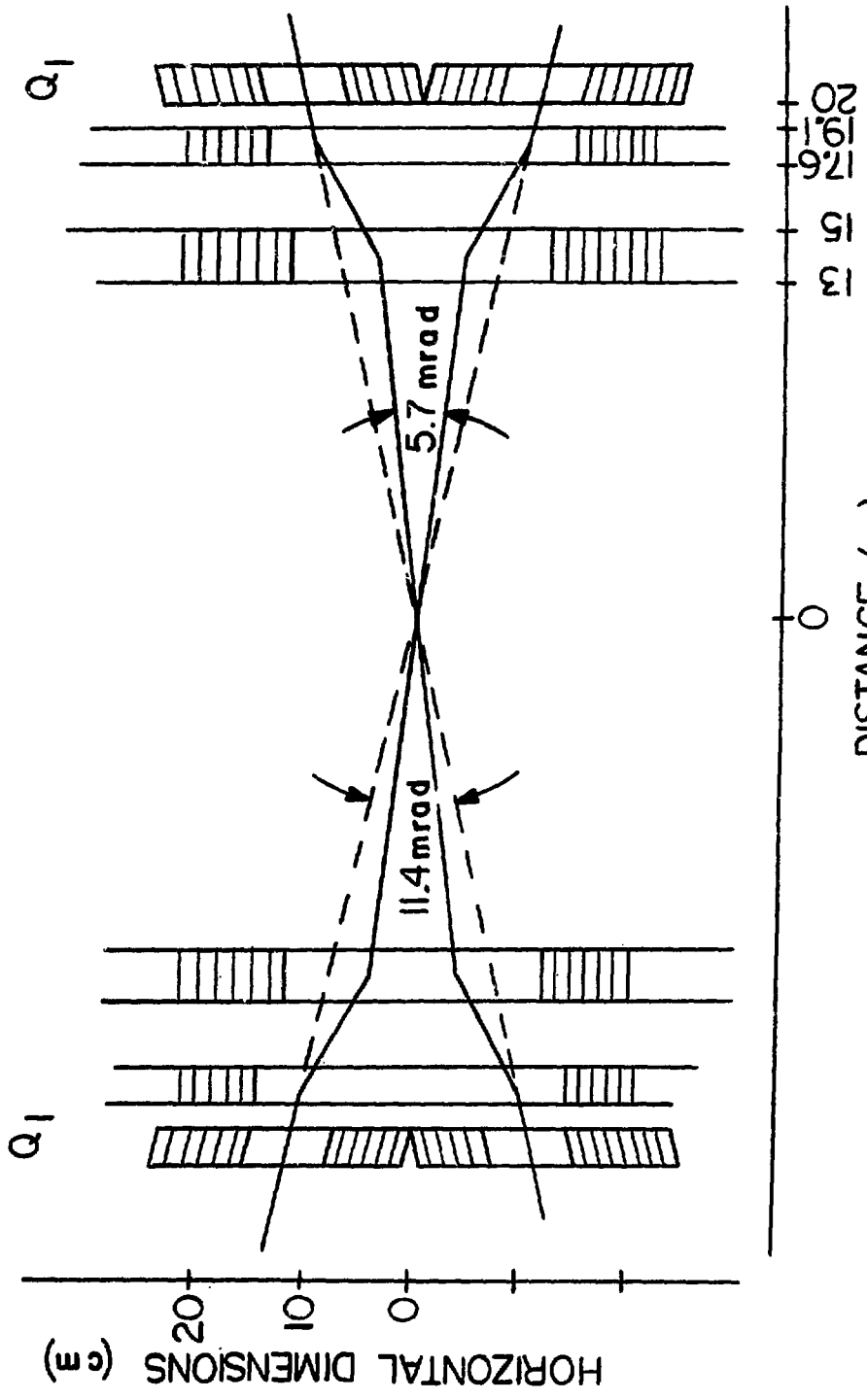

Fig. 11. Beam trajectories for high luminosity configuration. The crossing angle is reduced by a factor of two.

The luminosity and Tune Shift estimates are based on the following asymptotic expressions (that is, in the limit of large crossing angles):

$$L = \left(\frac{I}{e}\right)^2 \frac{1}{c\sqrt{\pi}\,\sigma_v^*\,\alpha} \tag{4.1}$$

$$\Delta\nu_v = \left(\frac{2}{\pi}\right)^{\frac{1}{2}} \frac{I}{ec} \frac{r_p \beta_v^*}{\gamma \sigma_v^* \alpha}\,, \tag{4.2}$$

$$\Delta\nu_h = 0 + \text{order } (1/\alpha^2)\,, \tag{4.3}$$

where I is beam current,

α is the total crossing angle,

σ_v^* is the rms vertical beam size at the crossing point,

γ is the energy in proton mass units,

β_v^* is the vertical β value at the crossing point,

and r_p is the classical proton radius ($=1.5 \times 10^{-18}$ m).

The interaction length for horizontal crossing can be estimated from

$$\ell_{\text{interaction}} = \pm \frac{4\sigma_h^*}{\alpha}\,, \tag{4.4}$$

where σ_h^* is the rms horizontal beam size at the crossing point.

With the ISA crossing design we are proposing, the long range beam-beam electromagnetic interaction is small, meaning that it is appropriate to use the asymptotic expressions for the tune shifts given above. The magnitude of the long range interaction strength is reflected in the "beam separation" parameter,

$$\eta = \beta_h^* \alpha / \sigma_h^* \tag{4.5}$$

where β_h^* is the horizontal β value at the crossing point, and σ_h^* is the horizontal beam size at the crossing point. For the hi-luminosity case of Table III, for example, the value of $\eta = 209.6$. The long range effect is strongest at low energy, where $\eta = 161.0$. Thus, we estimate that for the initial phase ISABELLE program, the contribution to the tune shifts from the long range interaction should be less than ½% of the vertical beam-beam tune shift.

The initial performance is predicated on the choice of crossing angle and stack current of 10 A. The significance of these parameters is reflected in the beam-beam tune shift which they produce under various conditions. Since the beam-beam tune shift is a measure of the beam-beam interaction and is positively correlated with radiation background in the experimental areas, it was deliberately chosen to have a small value. For example, the low-β configuration has $\Delta\nu \approx 9 \times 10^{-4}$, only about a factor of 2 larger than at the ISR. However, the nonlinear resonances which can be expected to produce beam loss, and so background, in a design with high periodicity, such as the ISA, are odd-ordered ones, and they are excited by random errors in the closed orbit positioning at the collision points. It is estimated that, at the tune shift levels proposed for the ISA, acceptable beam loss rates will result with orbit control at the collision points of about a tenth of a mm. With the present design, however, greater orbit precision could allow a larger tune shift and thus a luminosity larger than the design value. This could be obtained by a further reduction in the crossing angle, in the manner indicated in Fig. 11.

Acknowledgements

The author would like to thank D. Gilzinger and C. Briening for their valuable assistance in computing magnet coordinates and in completing the scaled drawings for the ISABELLE lattice.